Molecular interactions with CO_2 for controlling the regioselectivity of liquid phase hydrogenation of 2,4-dinitroaniline

Hiroshi Yoshida[a,c], Akitoshi Tomizawa[a], Hiroto Tachikawa[b], Shin-ichiro Fujita[a] and Masahiko Arai[a]

[a] Division of Chemical Process Engineering, Faculty of Engineering, Hokkaido University, Sapporo 060-8628, Japan
[b] Division of Materials Chemistry, Faculty of Engineering, Hokkaido University, Sapporo 060-8628, Japan
[c] Current address: Unit of Elements Strategy Initiative for Catalysts & Batteries, ESICB, Kyoto University, Kyoto 615-8510, Japan

Abstract: The catalytic hydrogenation of 2,4-dinitroaniline with a 0.5 wt% Pt/TiO_2 was investigated in a multiphase medium of tetrahydrofuran (THF) pressurized by CO_2 at different pressures and at 323 K. When CO_2 pressure was raised, the overall rate of hydrogenation simply decreased but the selectivity to the desired product of 4-nitro-1,2-phenylenediamine increased. The noticeable enhancement of the selectivity to 4-nitro-1,2-phenylenediamine can be explained by chemical actions of CO_2 molecules. *In situ* high-pressure FTIR and molecular simulations demonstrate that the dissolved CO_2 molecules may interact with amino group of the substrate and weaken the intra-hydrogen bonding between the amino and 2-nitro groups, which results in the change of the relative reactivity of the two nitro groups, yielding the desired product in a higher selectivity. The change of the intra- and inter-molecular interactions between the substrate and CO_2 molecules was theoretically examined by DFT calculation.

1. INTRODUCTION

When an organic liquid is pressurized by CO_2, its volume will expand to some extent depending on its properties and pressures. This liquid is often called as CO_2-dissolved expanded liquid phase (CXL). The solvent properties of a CXL may widely be tuned by CO_2 pressure, going from its pure liquid through dense phase CO_2-like liquid. The CXL has advantageous features as a reaction medium compared to conventional organic solvents and supercritical CO_2. Several review articles demonstrate interesting results of organic synthetic reactions in CXLs, including hydrogenation, oxidation, hydroformylation, and others.[1-5] Note that CXLs also serve an interesting medium for reactions including no gaseous reactants like Heck coupling and Diels-Alder reactions.[6] One of interesting actions of CO_2 in CXLs is the interaction with functional groups of organic substrates and/or reaction intermediates, which would accelerate or retard the reaction rate and change the product distribution. The authors show the significance of molecular interactions of CO_2 in the catalytic selective hydrogenation of α, β-unsaturated aldehydes to saturated alcohols[7, 8] and of nitro arenes to anilines[9, 10]. In the latter, for example, 100% selectivity to anilines can be achieved at any conversion level up to 100% total conversion with supported nickel catalysts. The interactions of CO_2 molecules with carbonyl and nitro groups are a significant factor determining the final product selectivity in these hydrogenation reactions. The interactions of CO_2 with functional groups of various organic compounds were measured by *in situ* high-pressure Fourier transform infrared spectroscopy (FTIR) in transmittance and attenuated total reflection (ATR) modes.[11, 12] Those results indicate that CO_2 molecules would act as a reaction promoter in CXLs more effectively than expected simply from its inertness nature. It is interesting and significant, therefore, to study the features and usefulness of CXLs for other more difficult organic synthetic reactions.

In this work, the regioselective hydrogenation of 2,4-dinitroaniline **1** has been investigated with a Pt/TiO_2 catalyst in a CXL using tetrahydrofuran (THF). The substrate includes two nitro groups at different positions (in different chemical environments) and so the authors expect that these nitro groups would interact with the dissolved CO_2 molecules and their reactivity would be changed in different modes. This would result in a change in the product selectivity (Scheme 1) as compared to the reference hydrogenation under conventional conditions in the presence of pressurized H_2 alone. Alaimo and Storrin previously reported that a high selectivity (> 90%) to 4-nitro-1,2-phenylenediamine **2** was achieved by the catalytic hydrogenation of **1** with heterogeneous catalysts of PtO_2, 5 wt% Rh/Al_2O_3, and 5 wt% Rh/C in dimethylformamide at 0.28 MPa initial pressure, in which, however, the addition of such a base as NH_4OH was necessary.[13] The product **2** is one of commercially important compounds, which can find practical utility in several fine chemical industries.[13] Since the work of Alaimo and Storrin in 1981, we can find few works on the selective hydrogenation of **1** to **2** using heterogeneous catalysts. Recently, Pagliaro and coworkers investigated chemoselective hydrogenation of various functionalized nitroarenes over heterogeneous Pd and Pt catalysts.[14, 15] However, the authors did not notice the regioselective hydrogenation of **1** to **2** in their works.

Scheme 1

The present authors have investigated the regioselective hydrogenation of **1** to **2** using a Pt/TiO_2 catalyst in THF pressurized by CO_2 at different pressures in this work and the influence of dense phase CO_2 on the reaction rate and the product selectivity has been examined. The interactions between the nitro and amino groups of the substrate **1** and CO_2 molecules dissolved in the solvent have been measured by *in situ* high-pressure FTIR in ATR mode for the liquid mixture of **1** and CO_2 in THF at different CO_2 pressures. Intra- and inter-molecular interactions should be operated[16-18] and would be modified by the presence of CO_2 molecules in the liquid phase. These molecular interactions have also been evaluated by molecular simulations assuming simple molecular structures of **1** coordinated to different numbers of CO_2 molecules. On the basis of those experimental and theoretical results, a noticeable (desirable) change in the product selectivity of hydrogenation of **1** to **2** by CO_2 pressurization has been discussed in detail.

2. EXPERIMENTAL AND THEORETICAL METHODS

2.1. Catalyst Preparation and Materials

A catalyst of 0.5 wt% Pt/TiO_2 was prepared by impregnation using TiO_2 (anatase/rutile = 7/3, BET surface area 49 m^2/g, Catalysis Society of Japan, JRC-TIO4(2)) and H_2PtCl_6 (Wako). The Pt-loaded TiO_2 sample was dried in ambient atmosphere at 373 K for 5 h and reduced in a 4% H_2 (N_2 balance) stream at 473 K for 3 h. The metal dispersion in the reduced sample measured by CO chemisorption was 10%.

2.2. Hydrogenation

A substrate of 2,4-dinitroaniline **1** and a solvent of THF were purchased from Wako and used as received. Among a few solvents tested, THF was selected since it was a good solvent for dissolving a certain amount of **1**. The hydrogenation of **1** was conducted in a 50 cm^3 stainless steel autoclave, to which the substrate (0.50 g), THF (10 cm^3), and catalyst (20 mg) were charged and the reactor was flushed with CO_2 three times to remove the air. After the reactor was heated up to 323 K, H_2 (4 MPa) was introduced and then liquid CO_2 was also introduced into the reactor with a high-pressure liquid pump (JASCO SCF-Get) to the desired pressure. The reaction was conducted while stirring the reaction mixture with a magnetic stirrer. After the reaction, the reactor was cooled with an ice-water bath and then depressurized carefully, and the composition of reaction mixture was analyzed by a gas chromatograph (GL Science GC-4000) using a capillary column (Zebron ZB-5) and a flame ionization detector. The total conversion of **1** was determined from the final amount of **1** unreacted divided by the initial amount of **1** loaded. The selectivity to a product was determined from the amount of the product formed divided by the total amount of products formed. To clarify the influence of functional group, 2,4-dinitrochlorobenzene **5** having chloro group instead of amino group was also used as a substrate of the hydrogenation reaction (Scheme 1).

2.3. High-pressure FTIR Measurement

Molecular interactions of CO_2 with the substrate of either **1** or **5** were examined by *in situ* high-pressure FTIR measurements using a JASCO FTIR-620 spectrometer with a triglycine sulfate detector with a wavenumber resolution of 2 cm^{-1}. The FTIR spectra were collected at 323 K (reaction temperature) for the CO_2-dissolved expanded THF phase by ATR mode using a home-designed cell of about 1 cm^3. It was loaded with a liquid mixture of the substrate and THF in the same concentrations as used in the reaction, purged with CO_2 three times, and loaded with liquid CO_2 up to the desired pressure. The temperature was adjusted to 323 K by resistivity heating with coils embedded in the cell. The experimental setups and detailed procedures are described elsewhere.[19] For better understanding, the same experiments were carried out with either 2- or 4-nitroaniline dissolved in THF to examine the molecular interactions of CO_2 molecules with 2- and 4-nitro groups in the substrate of **1**.

2.4. Phase Behavior Observation

The volume expansion of THF on CO_2 pressurization at different pressures was measured with a 10 cm^3 high pressure view cell equipped with two sapphire windows.[8-

[10] The cell was loaded with 2 cm^3 solvent, it was purged with CO_2 three times, and then it was heated up to a temperature of 323 K while stirring. After the desired temperature was obtained, 4 MPa H_2 was introduced, compressed CO_2 was fed into the cell to the desired pressure, and then stirring was stopped after 2 min. The volume of the liquid phase was then measured.

2.5. Molecular Simulations

Density functional theory (DFT) calculations were performed with the Gaussian 03 and 09 program packages.[20,21] The structures of clusters composed of nitro aromatic compounds and CO_2 were fully optimized at the B3LYP/6-311G(d,p) level.[22-24] in order to obtain sufficiently accurate energetics. Harmonic vibrational frequencies at the stationary points of clusters were calculated to check the local minima of the structures.

3. RESULTS AND DISCUSSION

3.1. Hydrogenation

Typical time profiles of total conversion and product selectivity are given in Figure 1. The two products of 4-nitro-1,2-phenylenediamine **2** and 2-nitro-1,4-phenylenediamine **3** were observed to form without any other byproducts (Scheme 1). The formation of 1,2,4-triaminobenzene **4** was not observed in the present work. As shown in Figure 1, the product selectivity did not change so much with conversion and this trend was also confirmed at different CO_2 pressures examined. The influence of CO_2 pressure on the overall conversion of **1** is presented in Figure 2. Unfortunately, the conversion was rapidly decreased by CO_2 pressurization in the range of pressures lower than 2 MPa and then gradually decreased with increasing CO_2 pressure at 2 - 8 MPa. Generally, in liquid phase hydrogenation reactions in the presence of H_2 and CO_2 at high pressures over supported metal catalysts, CO is formed and adsorbed on the surface of metal catalysts, often causing their undesired deactivation.[25,26] Therefore, a reaction run was also conducted with a catalyst sample on which CO was pre-adsorbed by exposure to 1% CO gas at 0.1 MPa for 10 min. The same product distribution as observed with untreated Pt/TiO_2 catalyst was obtained and no catalyst deactivation occurred, indicating that CO formed and adsorbed on the surface of Pt/TiO_2 under the present reaction conditions is not responsible for the reaction rate and the product selectivity.

Figure 1, Figure 2

The decrease of reaction rate with CO_2 pressure was also observed in the hydrogenation of 2-nitroaniline (2NA) and 4-nitroaniline (4NA) as shown in Figure 3. It is known that a significant amount of CO_2 is dissolved in the liquid phase and this may cause the decrease in the conversion for several multiphase reactions under dense phase CO_2. When the present reaction mixture was pressurized by CO_2, the volume of THF was gradually increased with increasing pressure up to 6 MPa by the dissolution of CO_2 and then rapidly increased at pressures from 6 MPa to 8 MPa (Figure 4). Finally, the reaction mixture formed a single gas phase at a pressure of 8.2 MPa. In the previous hydrogenation of nitrostyrene in CO_2-expanded solvent with Pt/TiO_2 catalyst at 323 K, the overall rate of hydrogenation was also decreased with increasing CO_2 pressure.[12] However, such a rapid decrease of conversion at lower CO_2 pressures than 2 MPa (Figures 2, 3) was not observed in our previous work, in which the reaction conditions such as the concentration of substrate, the volume expansion of solvent, and the amount of catalyst used were similar. From these results, the chemical interaction of dissolved CO_2 molecules with **1** seems to affect the reaction rate while the dilution effect of CO_2 is not so significant for the decrease in the overall conversion of **1**.

Figure 3, Figure 4

For the selectivity to the desired product **2**, on the other hand, an interesting effect of CO_2 pressurization was observed to appear. The selectivity to **2** is also plotted against CO_2 pressure in Figure 2. The selectivity to **2** was 76% in neat THF; it is noteworthy that it was enhanced by about 10% at a CO_2 pressure of 4 MPa, indicating that the regioselectivity of the hydrogenation of **1** to **2** was increased on the simple pressurization of CO_2. This result was contrary to the case of mono-nitro compounds of 2NA and 4NA, in which the hydrogenation of 2-nitro group in 2NA was suppressed to a larger extent by CO_2 pressurization compared to 4-nitro group in 4NA (Figure 3). These results imply that the chemical interactions of dissolved CO_2 molecules with 2,4-dinitroaniline **1** is different from those of 2NA and 4NA, which will be discussed later.

For better understanding of those results with **1**, the hydrogenation of 2,4-dinitrochlorobenzene **5**, 2-chloronitrobenzene and 4-chloronitrobenzene were also examined in the absence and presence of CO_2. The substrates of **5** was hydrogenated to 2-chloro-5-nitroaniline **6** and 4-chloronitroaniline **7**, and the fully-hydrogenated product of 6-chloro-1,3-phenylenediamine **8** was obtained in the present reaction (Scheme 1). In contrast to the case of **1** in Figure 2, the hydrogenation of **5** was accelerated with increasing CO_2 pressure while the selectivity to **6** and **7** remained unchanged (Figure5). Namely, the effects of CO_2 pressurization on the hydrogenation rate and the product selectivity were entirely different between **1** and **5**. In the hydrogenation of mononitro compounds of 2-chloronitrobenzene and 4-chloronitrobenzene in THF, the overall conversion was gradually decreased with increasing CO_2 pressure in the same manners irrespective of the relative positions of chloro and nitro groups (Figure 6). These results indicate that the overall reaction rate can be controlled by CO_2 pressurization but the product distribution is not affected in the hydrogenation of nitroarenes having chloro group. Therefore, the presence of adjacent amino group is significant for the appearance of CO_2 pressurization effect on the controlling of the product distribution in the hydrogenation of **1**. As mentioned above, the fully hydrogenated product of **4** was not observed in the present reaction system, which indicates that the difference of the reactivity between 2-nitro and 4-nitro groups in **1** significantly affect the product distribution. Therefore, we think that the structure around these nitro groups of **1** in the absence and presence of CO_2 is one of the most important factors to determine the reactivity of them and to clarify the effect of CO_2 pressurization as observed in the present work. In the following, detailed discussion about the impact of CO_2 molecules will be made using the results of *in situ* high-pressure FTIR and molecular simulations.

Figure 5, Figure 6

3.2. FTIR under Ambient Conditions

Reference data were collected for a THF - **1** mixture by transmittance FTIR, in which a liquid film sandwiched by KBr plates was measured under ambient conditions. 2NA, 4NA, nitrobenzene (NB), aniline (AN), as described in Scheme 2, and the mixture of NB and AN dissolved in THF were also subjected to the FTIR measurement (Figure 7), and the assignment of the absorption bands observed is given in Table 1. For 2NA, the absorption bands of asymmetric and symmetric stretching vibration modes of nitro group, $\nu_{as}(NO_2)$ and $\nu_s(NO_2)$, are located at 1505 cm^{-1} and 1340 cm^{-1}, respectively (Figure 7a). For 4NA, the same absorption bands appear but at different frequencies, 1494 cm^{-1} for $\nu_{as}(NO_2)$ and 1325 cm^{-1} for $\nu_s(NO_2)$. The latter one is seen as a shoulder peak of another clear peak, which is assigned to stretching vibration modes of C–NH_2 bond. For the substrate **1**, a large band at 1329 cm^{-1} is assigned to $\nu_s(NO_2)$ of 2- and 4-nitro groups and a weak band at 1513 cm^{-1} is assigned to $\nu_{as}(NO_2)$ of 2-nitro group. A shoulder band at about 1484 cm^{-1} may be assigned to the absorption of $\nu_{as}(NO_2)$ of 4-nitro group. The peak frequency and the relative intensity of absorption bands of nitro group are different depending on the structure of the three nitroarenes examined, which would indicate different modes and extents of intra- and inter-hydrogen bonding.[16, 27, 28] From the comparison of the FTIR spectra of NB and the mixture of NB and AN, the absorption bands at 1526 cm^{-1} for $\nu_{as}(NO_2)$ and 1347 cm^{-1} for $\nu_s(NO_2)$ were not shifted even in the presence of AN, indicating that the influence of inter-hydrogen bonding between nitro group and amino group is weak and the peak position of $\nu(NO_2)$ is mainly affected by intra-hydrogen bonding or other intra-molecular interactions.

Figure 7

Figure 7b displays the spectra for the range of stretching vibration of amino group for three nitroarenes, NB, AN, and the mixture of NB and AN. The assignment of these bands is also shown in Table 1. The spectra of 4NA is similar to that of AN, in which three absorption bands are located at 3472 cm^{-1}, 3349 cm^{-1} and 3224 cm^{-1}. The former two bands are assignable to asymmetric and symmetric stretching vibration modes, $\nu_{as}(NH_2)$ and $\nu_s(NH_2)$.[18] The peak intensity of the latter band of **1** at around 3200 cm^{-1} is relatively stronger than that of AN, and the same trend can be seen with the absorption bands of **1** and 2NA. Therefore, the relative peak intensity of the absorption band of $\nu_s(NH_2)$ located around 3200 cm^{-1} should imply the inter-hydrogen bonding interaction between H atom of amino group and O atom of nitro group of another molecule. For **1** and 2NA, three absorption bands are also observed, similar to 4NA and AN**,** but the peak frequency and the relative intensity of the absorption bands are different. The peak position of the absorption band at 3453 cm^{-1} corresponds with that of 4NA and AN, whereas the other two absorption bands appeared at a frequency lower by about 30 cm^{-1} compared with 4NA and AN. These results can be explained using DFT calculation, as will be discussed later. It is noted again that, for the substrate **1** of our interest, both intra- and inter-hydrogen bonding interactions should exist under ambient conditions.

3.3. FTIR under High Pressure CO_2 Conditions

The substrate of **1**, 2NA and 4NA were also used in *in situ* high-pressure FTIR-ATR measurement at 323 K. Figure 8 shows the FTIR spectra in the range of $\nu(NO_2)$ collected at different CO_2 pressures. The reference data given in Figure 7 and Table 1 were used to assign the absorption bands observed with **1**, 2NA and 4NA under high CO_2 pressure conditions. For each of these anilines, the strength of absorption decreased with increasing CO_2 pressure due to the dilution effect. For 2NA in Figure 8b, the absorption bands of $\nu_{as}(NO_2)$ and $\nu_s(NO_2)$ are located at the same frequencies at 1505 cm^{-1} and 1340 cm^{-1}, respectively, irrespective of CO_2 pressure. Similar results were obtained for 4NA that two absorption bands of $\nu_{as}(NO_2)$ at 1505 cm^{-1} and $\nu_s(NO_2)$ at 1340 cm^{-1} were little shifted with increasing CO_2 pressure (Figure 8c). These results may indicate that there is no or little direct molecular interaction between dissolved CO_2 molecule and nitro group of 2NA and 4NA. In our previous works, clear peak-shift was observed for the absorption band of $\nu_{as}(NO_2)$ and $\nu_s(NO_2)$ in the case of NB[9] and NS[12]; therefore, the presence of amino group in the molecule may prevent or weaken the direct interaction between CO_2 molecule and nitro group of 2NA and 4NA, which may be caused by inter- or intra-hydrogen bonding with H atom of amino group and O atom of nitro group. However, for the substrate **1**, the absorption band of $\nu_{as}(NO_2)$ of 2-nitro group at 1513 cm^{-1} becomes weakened with CO_2 pressure and the absorption band of $\nu_{as}(NO_2)$ of 4-nitro group at 1484 cm^{-1} clearly increased while remaining its frequency, implying that the peak frequency of 2-nitro group was selectively red-shifted with increasing CO_2 pressure among two nitro groups of the substrate of **1**. Therefore, we concluded that the relative reactivity of 2-nitro group against that of 4-nitro group was enhanced by CO_2 pressurization, resulting in the increase of the selectivity to **2** (Figure 2). This change was not observed in the FTIR measurements for **1** in THF with different concentrations at ambient pressures and the absorption band of $\nu_{as}(NO_2)$ of 2-nitro group simply decreased with decreasing concentration of **1** without increase in the absorption band of $\nu_{as}(NO_2)$ of 4-nitro group (SI, Figure S1). These results suggest that the dilution of reaction mixture by CO_2 dissolution is not the cause of above-mentioned spectra change and CO_2 molecules may chemically influence the substrate of **1**.

Figure 8

Figure 9 shows the FTIR-ATR spectra in the range of the amino group for three nitroarenes. In contrast to the case of nitro group in Figure 8, remarkable changes can be seen for 2NA (Figure 9b) but not for 4NA (Figure 9c). For 2NA, the absorption band of $\nu_{as}(NH_2)$ at 3471 cm^{-1} became weakened with CO_2 pressure and was a little blue-shifted. There are two absorption bands assigned to $\nu_s(NH_2)$ at a main peak of 3326 cm^{-1} and a shoulder peak of 3368 cm^{-1} under ambient condition. Under CO_2 pressurized conditions, the peak intensity of the former decreased while that of the latter increased. In addition, the peak frequency of $\nu_s(NH_2)$ at 3368 cm^{-1} was gradually blue-shifted to 3378 cm^{-1} with increasing CO_2 pressure up to 12 MPa. The absorption band of $\nu_s(NH_2)$ for AN and 4NA appeared at a higher frequency compared with that for 2NA as shown in Figure 7b, suggesting that the intra-molecular hydrogen bonding interaction between nitro and amino group in 2NA weakened the peak frequency of $\nu_s(NH_2)$ in the absence of CO_2, and this interaction was canceled by CO_2 pressurization. Such a peak shift was not observed for 4NA and the peak intensity simply decreased with increasing CO_2 pressure due to dilution effect (Figure 9c). For the substrate **1**, the absorption band of $\nu_s(NH_2)$, which was observed at 3312 cm^{-1} under ambient condition, was slightly blue-shifted similar to the case of 2NA whereas the extent of the peak shift was ca. 13 cm^{-1} (Figure 9a), which was much smaller than 52 cm^{-1} for 2NA (Figure 9b). One can say that the presence of 4-nitro group in **1** may suppress the peak shift of $\nu(NH_2)$ in the presence of compressed CO_2. These results strongly suggest that amino group of **1** has the interaction with dissolved CO_2 molecule and it is weaker compared with the case of 2NA because of the presence of 4-nitro group. Several researchers note that 4NA is well stabilized by the formation of the resonance structure but this is not the case in 2NA.[29-31] Namely, we could not observe any interactions between CO_2 and 4NA because of strong resonance structure (Figure 8c, 9c) but the direct interaction of CO_2 with **1** and 2NA was observed (Figure 9a, 9b). The peak intensity of amino group in the substrate **1** increased with CO_2 pressurization (Figure 9a), which was contrary to the other FTIR spectra. In the absence of CO_2, **1** exits in the form of dimer through inter-hydrogen bonding between 2-nitro and amino groups. In the presence of CO_2, however, CO_2 molecules approach to and break the dimer into the monomers and some CO_2 molecules are coordinated to the amino group of **1**. The inter-hydrogen bonding weakens and so the strength of N-H bonds increases, as estimated from the blue-shift observed. The molecular interactions with CO_2 should result in a variation in the electronic structure of around the amino group, which might cause an increase in the strength of the absorption band with CO_2 pressure.

Figure 9

From the comparison of FTIR results among **1**, 2NA and 4NA under high-pressure CO_2 conditions, the influence of CO_2 pressurization on the reactivity of 2- and 4-nitro group of **1** can be discussed. The presence of amino group in the structure of 2NA and 4NA suppress the peak shift of $\nu(NO_2)$ even at high CO_2 pressure, which is different from the case of NB[9]. For **1**, however, only a red shift of $\nu(NO_2)$ of 2-nitro group was observed with increasing CO_2 pressure whereas $\nu(NO_2)$ of 4-nitro group was located at the same frequency (Figure 8). On the other hands, the peak position of $\nu(NH_2)$ did not change by CO_2 pressurization for 4NA whereas those for **1** and 2NA were blue-shifted (Figure 9), and the order of the extent of peak shift was 2NA > **1** > 4NA. These results indicate that the direct molecular interaction between amino group of **1** and dissolved CO_2 molecules affect the reactivity of 2-nitro group, resulting in the increase of the selectivity to **2** as shown in Figure 2. For 2NA, CO_2 species can coordinate to the NH_2 group (Figure 9) and this may cause a steric effect on the adjacent NO_2 group. Such a steric effect cannot appear for 4NA. Thus, the negative impact of CO_2 pressurization should be larger for 2NA than for 4NA. For **1** of our interest, a similar negative impact of CO_2 molecules should exist for 4-nitro group. For 2-nitro group, however, there is observed a red-shift of $\nu(NO_2)$ (Figure 8a), which is a positive effect (increasing its reactivity). The above-mentioned negative steric effect on the 2-nitro group caused by the coordination of CO_2 species to the adjacent NH_2 group may be offset to some extent. Thus, the negative effect of CO_2 pressurization should be smaller for the 2-nitro group than for the 4-nitro group, resulting in the increase in the selectivity to the hydrogenation of the former 2-nitro group. We measured *in situ* high-pressure FTIR-ATR using 2,4-dinitrochlorobenzene **5** in THF to determine the interaction of CO_2 pressurization on two nitro groups of **5** but no peak-shift was observed (SI, Figure S2), which also supports the indirect interaction of dissolved CO_2 with 2-nitro group of **1** via amino group. To clarify this indirect molecular interaction of dissolved CO_2 molecules with the substrate, the local structures of **1**, 2NA and 4NA in the absence and presence of CO_2 molecules were examined by molecular simulations.

3.4. Molecular Simulations

In addition to the above-mentioned FTIR measurements, intra- and inter-interactions that should occur with substrates and CO_2 molecules have theoretically been studied by molecular simulations. The dissolved CO_2 molecules approach in closer proximity to the substrate than the solvent THF molecules and may form a cluster with **1** in the present reaction system. The optimized structure of the cluster with **1** and CO_2 molecules were calculated and the clusters of **1** coordinated with four or five CO_2 molecules were obtained as the most stabilized CO_2-coordinated clusters in THF (Figure 10). It was calculated that NO bonding distances of 2- and 4-nitro groups in the absence of CO_2 are 1.220, 1.238 Å and 1.224, 1.226 Å, respectively, and these NO distances are hardly changed when the substrates of **1** was clustered with four or five CO_2 molecules (Figure 10b and 10c). The same results were obtained for NO bonding distance of 2- and 4-nitro groups in chloro-2,4-dinitrobenzene **5** (SI, Figure S3), and hence, we can say that there is no or little direct interactions of dissolved CO_2 molecules with the NO group in the substrates. However, a significant change can be seen in the distance between O atom of 2-nitro group and H atom of amino group, which may form the intra-hydrogen bonding in **1**. The distance between O and H is 1.906 Å in the absence of CO_2 (Figure 10a) and it is extended to 1.945 and 1.952 Å when the CO_2-coordinated clusters are formed (Figure 10b, 10c), which clearly indicates that the intra-hydrogen bonding between 2-nitro group and amino group in **1** is weakened by the coordination of CO_2 around **1**. It is well known that an amine species has strong affinity with CO_2[32,33] and it may cause the suppression of intra-hydrogen bonding, resulting in the increase of the reactivity of 2-nitro group in **1** as above-mentioned in Figure 2. The structures of CO_2-coordinated clusters of 2NA and 4NA with three and four CO_2 molecules were also calculated using DFT simulations (Figure 11). In accordance with the case of **1**, the bonding distance of intra-hydrogen bonding in 2NA is extended from 1.910 Å to 1.937 Å with CO_2 coordination whereas NO bonds of 2-nitro group in 2NA and of 4-nitro group in 4NA remain unchanged even in the presence of CO_2 molecules. The extension of intra-hydrogen bonding due to CO_2 coordination is relatively larger in **1** with four CO_2 molecules (0.039 Å) and with five CO_2 molecules (0.046 Å) compared with that in 2NA with three CO_2 molecules (0.027 Å), which may cause the peak-shift of NO stretching vibration of **1** (Figure 8a).

Figure 10, Figure 11

The dimerization of **1** due to inter-hydrogen bonding in THF can occur and, therefore, we also examined the interaction of CO_2 with the dimer of **1**. Figure 12a shows the optimized structure of dimers of 2NA, for which the enthalpy of formation is calculated to be 29.3 kJ mol^{-1}. The dimer of 4NA was formed with different modes; O atoms of nitro group in 4NA form the inter-hydrogen bonding respective to with H atom of amino group and H atom of aromatic ring (Figure 12b). The enthalpy of formation for the dimer of 4NA is 35.6 kJ mol^{-1}, which is larger compared with that of 2 NA, indicating that the appropriate structure of the dimer of **1** can be assumed as in Figure 13. The bonding distance of intra-hydrogen bond in the dimer of **1** is calculated to be 1.984 Å in the absence of CO_2 (Figure 13a), which is much longer compared with that of monomer of 1.906 Å. It is a little shortened to 1.980 Å with the coordination of eight CO_2 molecules as shown in Figure 13b, which is different from the result of monomer. The bonding energy of CO_2 molecule on the cluster is calculated to be 9.20 kJ mol^{-1}, and this value is much lower than the enthalpy of formation of dimers. Interestingly, the bonding distance of inter-hydrogen bond in the dimer of **1** is quite extended from 2.116 Å to 2.262 Å by CO_2 coordination, indicating that the dimerization is weakened and the state of **1** change from dimer to monomer. The formation of the dimer of **1** may cause a steric hindrance and inhibit the hydrogenation of 2-nitro group of **1**, and namely, one can say that the decomposition of the dimer due to CO_2 coordination enhances the reactivity of 2-nitro group, resulting in the increase of the selectivity to **2**, as observed in the present hydrogenation (Figure 2).

Figure 12, Figure 13

The results of DFT calculation for chloro-2,4-dinitrobenzene **5** were also given in Figure 14. The distance between two molecules of **5** is calculated to be 3.260 Å and it is much longer compared with 2.262 Å of **1** in Figure 13, suggesting that the dimerization is unlikely to occur in the case of **5**. Moreover, the bonding distances of NO in **5** are not affected by CO_2 coordination. These results indicate that the reactivity of two nitro groups in **5** is not affected by the interaction with CO_2 molecules, which corresponds to the reaction results in Figure 5.

Figure 14

3.5. Functions of CO_2 at High Pressures

The experimental and theoretical results obtained will allow us to explain the fact that CO_2 pressurization enhances the selectivity to **2** in hydrogenation of **1** in THF solvent as follows. The results of FTIR-ATR and molecular simulations suggest that there is no or little direct interaction of dissolved CO_2 molecules with nitro groups of **1** but the interaction between CO_2 molecule and amino group of **1** weakens the intra-hydrogen bonding between amino group and 2-nitro group. This indirect impact of CO_2 pressurization may enhance the reactivity of 2-nitro group and result in the increase of the selectivity to **2** in the presence of dense phase CO_2. These effects were also observed in 2NA and 4NA but not in chloronitro derivatives of **5**, 2CNB and 4CNB. Therefore, the use of dense phase CO_2 will be an interesting method for regioselective organic reactions by selectivity activating a substituent like nitro group in which its reactivity is masked by interactions with an adjacent functional group like amino group. It is worth investigating such a potential of CO_2 molecules as a reaction promoter in other different liquid phase organic synthetic reactions in the near future.

Although the selectivity to the hydrogenation of 2-nitro group of the substrate **1** is enhanced, the overall rate of conversion is lowered on CO_2 pressurization (Figure 2). The structure of 2,4-dinitroaniline dimer tends to break into monomer on CO_2 pressurization. From the FTIR results, the amino group strongly interacts with CO_2 molecules and this should cause a steric effect on the 2-nitro group but not on the 4-nitro group. There are also interactions of CO_2 species with the nitro groups and the CO_2 is assumed to decrease the reactivity of the 4-nitro group, similar to the case of nitrobenzene.[9] In contrast, the reactivity of the 2-nitro group is increased, judging from the red-shift of $\nu(NO_2)$

absorption band on CO_2 pressurization. This positive effect may be offset to some extent by the negative steric effect of CO_2 species coordinating to the adjacent amino group. The negative effect would be more significant and, as a result, the overall rate of conversion should decrease with increasing CO_2 pressure. As above-mentioned, however, the relative reactivity of the 2-nitro group is larger with respect to the 4-nitro group and thus the selectivity to the hydrogenation of the former NO_2 group is enhanced.

4. CONCLUSIONS

In the hydrogenation of 2,4-dinitroaniline **1** with a 0.5 wt% Pt/TiO_2 catalyst in CO_2-dissolved expanded tetrahydrofuran (THF) at 323 K and at a H_2 pressure of 4 MPa, 4-nitro-1,2-phenylenediamine **2** and 2-nitro-1,4-phenylenediamine **3** were observed to form. The overall rate of hydrogenation of **1** decreased with an increase in CO_2 pressure while the selectivity to the desired product **2** increased. In contrast to the selectivity to **2** of 76% in neat THF, it was enhanced by about 10% at 4 MPa. The noticeable enhancement of the selectivity to **2** was ascribable to interactions of the dissolved CO_2 molecules with the two nitro groups of **1** in different manners. These interactions caused a difference in the relative reactivity between 2-nitro and 4-nitro groups, as confirmed by *in situ* high-pressure FTIR and molecular simulations, which resulted in the improved regioselective hydrogenation of **1** to **2** in the presence of dense phase CO_2. The present results demonstrate an interesting function of CO_2 molecules as an effective controller in liquid phase reactions and the usefulness of CO_2-dissolved expanded liquid phases for organic synthetic reactions in which the product selectivity is a major concern.

■ ACKNOWLEDGEMENTS

This work was supported by Japan Society for the Promotion of Science with Grant-in-Aid for Scientific Research (B) 22360327 and JSPS Fellows 242667.

■ REFERENCES

(1) Hallett, J. P.; Kitchens, C. L.; Hernandez, R.; Liotta, C. L.; Eckert, C. A. *Acc. Chem. Res.* 2006, **39**, 531.
(2) Jessop, P. G.; Subramaniam, B. *Chem. Rev*. 2007, **107**, 2666.
(3) Kruse, A.; Vogel, H. Chem. *Eng. Technol.* 2008, **31**, 23.
(4) Akien, G. R.; Poliakoff, M. *Green Chem*. 2009, **11**, 1083.

(5) Arai, M.; Fujita, S.; Shirai, M. *J. Supercrit. Fluids* 2009, **47**, 351.

(6) Fujita, S.; Tanaka, T.; Akiyama, Y.; Asai, K.; Hao, J.; Zhao, F.; Arai, M. *Adv. Synth. Catal.* 2008, **350**, 1615.

(7) Bhanage, B. M.; Ikushima, Y.; Shirai, M.; Arai, M. *Catal. Lett*. 1999, **62**, 175.

(8) Zhao, F.; Fujita, S.; Akihara, S.; Arai, M. *J. Phys. Chem. A* 2005, **109**, 4419.

(9) Meng, X.; Cheng, H.; Akiyama, Y.; Hao, Y.; Qiao, W.; Yu, Y.: Zhao, F.; Fujita, S.; Arai, M. *J. Catal*. 2009, **264**, 1.

(10) Meng, X.; Cheng, H.; Fujita, S.; Hao, Y.; Shang, Y.; Yu, Y.; Cai, S.; Zhao, F.; Arai, M. *J. Catal*. 2010, **269**, 131.

(11) Akiyama, Y.; Fujita, S.; Senboku, H.; Rayner, C. M.; Brough, S. A.; Arai, M. *J. Supercrit. Fluids* 2008, **46**, 197.

(12) Yoshida, H.; Kato, K.; Wang, J.; Meng, X.; Narisawa, S.; Fujita, S.; Wu, Z.; Zhao, F.; Arai, M. *J. Phys. Chem. C* 2011, **115**, 2257.

(13) Alaimo, R. J.; Storrin, R. J. in "Catalysis of Organic Reactions", Moser, W. R. (Ed.), Dekker, New York, 1981, pp. 473.

(14) Pandarus, V.; Ciriminna, R.; Béland, F.; Pagliaro, M. *Catal. Sci. Technol.* 2011, **1**, 1616.

(15) Pandarus, V.; Ciriminna, R.; Béland, F.; Pagliaro, M. *Adv. Synth. Catal.* 2011, **353**, 1306.

(16) Nomura, M.; Nakata, S. *Nippon Kagaku Kaishi*, 1990, 48.

(17) Panunto, T. W.; Urbánczyk-Lipkowska, Z.; Johnson, R.; Etter, M. C. *J. Am. Chem. Soc.* 1987, **109**, 7786.

(18) Bellamy, L. J.; Williams, R. L. *Spectrochim. Acta*, 1957, **9**, 341.

(19) Fujita, S.; Yoshida, H.; Asai, K.; Meng, X.; Arai, M. *J. Supercrit. Fluids*, 2011, **60**, 106.

(20) Frisch, M. J.; Trucks, G. W.; Schlegel, H. B.; Scuseria, G. E.; Robb, M. A.; Cheeseman, J. R.; Montgomery, J. A., Jr.; Vreven, T.; Kudin, K. N.; Burant, J. C.; Millam, J. M.; Iyengar, S. S.; Tomasi, J.; Barone, V.; Mennucci, B.; Cossi, M.; Scalmani, G.; Rega, N.; Petersson, G. A.; Nakatsuji, H.; Hada, M.; Ehara, M.; Toyota, K.; Fukuda, R.; Hasegawa, J.; Ishida, M.; Nakajima, T.; Honda, Y.; Kitao, O.; Nakai, H.; Klene, M.; Li, X.; Knox, J. E.; Hratchian, H. P.; Cross, J. B.; Bakken, V.; Adamo, C.; Jaramillo, J.; Gomperts, R.; Stratmann, R. E.; Yazyev, O.; Austin, A. J.; Cammi, R.; Pomelli, C.; Ochterski, J. W.; Ayala, P. Y.; Morokuma, K.; Voth, G. A.; Salvador, P.; Dannenberg, J. J.; Zakrzewski, V. G.; Dapprich, S.; Daniels, A. D.; Strain, M. C.; Farkas, O.; Malick, D. K.; Rabuck, A. D.; Raghavachari, K.; Foresman, J. B.; Ortiz, J. V.; Cui, Q.; Baboul, A. G.; Clifford, S.; Cioslowski, J.; Stefanov, B. B.; Liu, G.; Liashenko, A.; Piskorz, P.; Komaromi, I.; Martin, R. L.;

Fox, D. J.; Keith, T.; Al-Laham, M. A.; Peng, C. Y.; Nanayakkara, A.; Challacombe, M.; Gill, P. M. W.; Johnson, B.; Chen, W.; Wong, M. W.; Gonzalez, C.; and Pople, J. A. Gaussian 03, Revision B.04; Gaussian, Inc.: Wallingford, CT, 2004. 374

(21) Frisch, M. J.; Trucks, G. W.; Schlegel, H. B.; Scuseria, G. E.; Robb, M. A.; Cheeseman, J. R.; Scalmani, G.; Barone, V.; Mennucci, B.; Petersson, G. A.; Nakatsuji, H.; Caricato, M.; Li, X.; Hratchian, H. P.; Izmaylov, A. F.; Bloino, J.; Zheng, G.; Sonnenberg, J. L.; Hada, M.; Ehara, M.; Toyota, K.; Fukuda, R.; Hasegawa, J.; Ishida, M.; Nakajima, T.; Honda, Y.; Kitao, O.; Nakai, H.; Vreven, T.; Montgomery, J. A., Jr.; Peralta, J. E.; Ogliaro, F.; Bearpark, M.; Heyd, J. J.; Brothers, E.; Kudin, K. N.; Staroverov, V. N.; Kobayashi, R.; Normand, J.; Raghavachari, K.; Rendell, A.; Burant, J. C.; Iyengar, S. S.; Tomasi, J.; Cossi, M.; Rega, N.; Millam, N. J.; Klene, M.; Knox, J. E.; Cross, J. B.; Bakken, V.; Adamo, C.; Jaramillo, J.; Gomperts, R.; Stratmann, R. E.; Yazyev, O.; Austin, A. J.; Cammi, R.; Pomelli, C.; Ochterski, J. W.; Martin, R. L.; Morokuma, K.; Zakrzewski, V. G.; Voth, G. A.; Salvador, P.; Dannenberg, J. J.; Dapprich, S.; Daniels, A. D.; Farkas, O.; Foresman, J. B.; Ortiz, J. V.; Cioslowski, J.; Fox, D. J. Gaussian 09, Revision A.1; Gaussian, Inc.: Wallingford, CT, 389, 2009.

(22) Becke, A. D. *J. Chem. Phys.* 1993, **98**, 5648.

(23) Lee, C.; Yang, W.; Parr, R. G. *Phys. Rev. B* 1988, **37**, 785.

(24) Stephens, P. J.; Devlin, F. J.; Chabalowski, C. F.; Frisch, M. J., *J. Phys. Chem.* 1994, **98**, 11623.

(25) Ferri, D.; Bürgi, T.; Baiker, A. *Phys. Chem. Chem. Phys.* 2002, **4**, 2667.

(26) Burgener, M.; Ferri, D.; Grunwaldt, J.-D.; Mallat, T.; Baiker, A. *J. Phys. Chem. B* 2005, **109**, 16794.

(27) Dyall, L. K. *Spectrochim. Acta.* 1961, **17**, 291.

(28) Dyall, L. K. *Spectrochim. Acta.* 1969, **25A**, 1727.

(29) Huse, G.; Powell, H. M.; J. Chem. Soc. 1940, 1398.

(30) Kamlet, M. J.; Adolph, H. G.; Hoffsommer, J. C.; J. Am. Chem. Soc. 1964, **86**, 4018.

(31) Macnicol, D. D.; Tetrahedron Lett. 1975, **30**, 2599.

(32) Xie, X.; Liotta, C. L.; Eckert, C. A. *Ind. Eng. Chem. Res.* 2004, **43**, 7907.

(33) Chatterjee, M.; Kawanami, H.; Sato, M.; Ishizaka, T.; Yokoyama, T.; Suzuki, T. *Green Chem.* 2010, **12**, 87.

Scheme and Figure Captions

Scheme 1. Reaction pathways in hydrogenation of 2,4-dinitroaniline and 2,4-dinitrochlorobenzene.

Figure 1. Time profiles of conversion and selectivity to **2** in hydrogenation of **1** using 0.5 wt% Pt/TiO_2 at 323 K and at a H_2 pressure of 4 MPa.

Figure 2. Influence of CO_2 pressure on the overall conversion and the selectivity to **2** in hydrogenation of **1** using 0.5 wt% Pt/TiO_2 for 1 h at 323 K and at a H_2 pressure of 4 MPa.

Figure 3. The change of total conversion of 2-nitroaniline (2NA) and 4-nitroaniline (4NA) on CO_2 pressurization at 323 K in the presence of 4 MPa H_2.

Figure 4. The extent of volume expansion of THF liquid phase on CO_2 pressurization at 323 K in the presence of 4 MPa H_2.

Figure 5. Influence of CO_2 pressure on the overall conversion and selectivity to **6** and **7** in hydrogenation of **5** using 0.5 wt% Pt/TiO_2 for 30 min at 323 K and at a H_2 pressure of 4 MPa.

Figure 6. The change of total conversion of 2-chloronitrobenzene (2CNB) and 4-chloronitrobenzene (4CNB) on CO_2 pressurization at 323 K in the presence of 4 MPa H_2.

Scheme 2. Substrates used for FTIR measurements.

Figure 7. FTIR spectra in the ranges of (a) 1200 – 1700 cm^{-1} (NO_2) and (b) 3100 – 3600 cm^{-1} (NH_2) for 2,4-dinitroaniline **1**, 2-nitroanilline, 4-nitroaniline, nitrobenzene (NB), aniline (AN) and the mixture of NB and AN dissolved in THF measured in transmittance mode under ambient conditions.

Table 1. Assignment of absorption bands observed for **1**, 2NA, 4NA, NB and AN in THF under ambient conditions.

Figure 8. High-pressure FTIR spectra in the range of $\nu(NO_2)$ for (a) **1**, (b) 2-nitroaniline and (c) 4-nitroaniline dissolved in THF measured in ATR mode at 323 K at 4 MPa of H_2 and different CO_2 pressures given.

Figure 9. High-pressure FTIR spectra in the range of $\nu(NH_2)$ for (a) **1**, (b) 2-nitroaniline and (c) 4-nitroaniline dissolved in THF measured in ATR mode at 323 K at 4 MPa of H_2 and different CO_2 pressures given.

Figure 10. The optimized structures of CO_2-coordinated clusters of **1** with four CO_2 molecules (b) and five CO_2 molecules (c) and the bonding distances of NO of nitro groups and intra-hydrogen bonding between 2-nitro group and amino group in **1**. The values are in Å.

Figure 11. The optimized structures of 2NA (a), CO_2-coordinated clusters of 2NA with three CO_2 molecules (b), 4NA (c), and CO_2-coordinated clusters of 4NA with four CO_2 molecules (d). The bonding distances of NO of nitro groups and intra-hydrogen bonding between 2-nitro group and amino group in 2NA are given in Å.

Figure 12. The optimized structures of the dimer of 2NA (a) and 4NA (b). The values of bonding distances are in Å.

Figure 13. The optimized structures of the dimer of 2,4-dinitroaniline **1** (a) and CO_2-coordinated cluster with eight CO_2 molecules (b). The bonding distances of NO of nitro groups, intra-hydrogen bonding between 2-nitro group and amino group in **1** and inter-hydrogen bonding in the cluster are given in Å.

Figure 14. The optimized structures of the dimer of chloro-2,4-dinitrobenzene **5** forming the cluster with eight CO_2 molecules. The bonding distances of NO of nitro groups and the distance between two substrates are given in Å.

Scheme, Figure, and Table in the order of appearance:

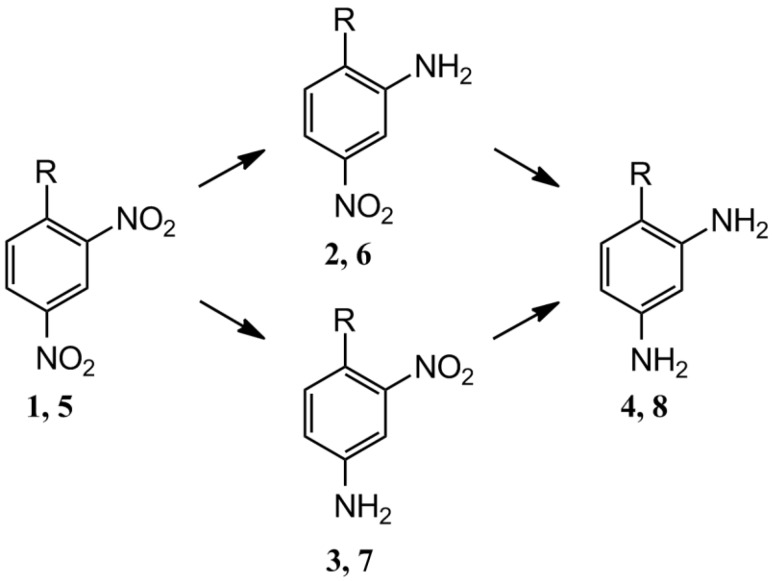

$R = NH_2$

1: 2,4-Dinitroaniline | **2**: 4-Nitro-1,2-phenylenediamine

3: 2-Nitro-1,4-phenylenediamine | **4**: 1,2,4-Triaminobenzene

$R = Cl$

5: 2,4-Dinitrochlorobenzene | **6**: 2-Chloro-5-nitroaniline

7: 4-Chloro-3-nitroaniline | **8**: 6-Chloro-1,3-phenylenediamine

Scheme 1. Reaction pathways in hydrogenation of 2,4-dinitroaniline and 2,4-dinitrochlorobenzene.

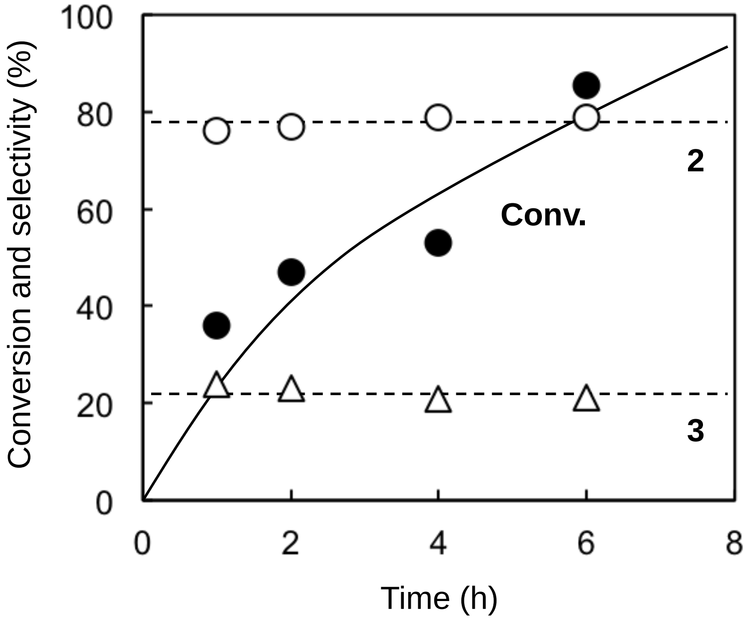

Figure 1. Time profiles of conversion and selectivity to **2** in hydrogenation of **1** using 0.5 wt% Pt/TiO_2 at 323 K and at a H_2 pressure of 4 MPa.

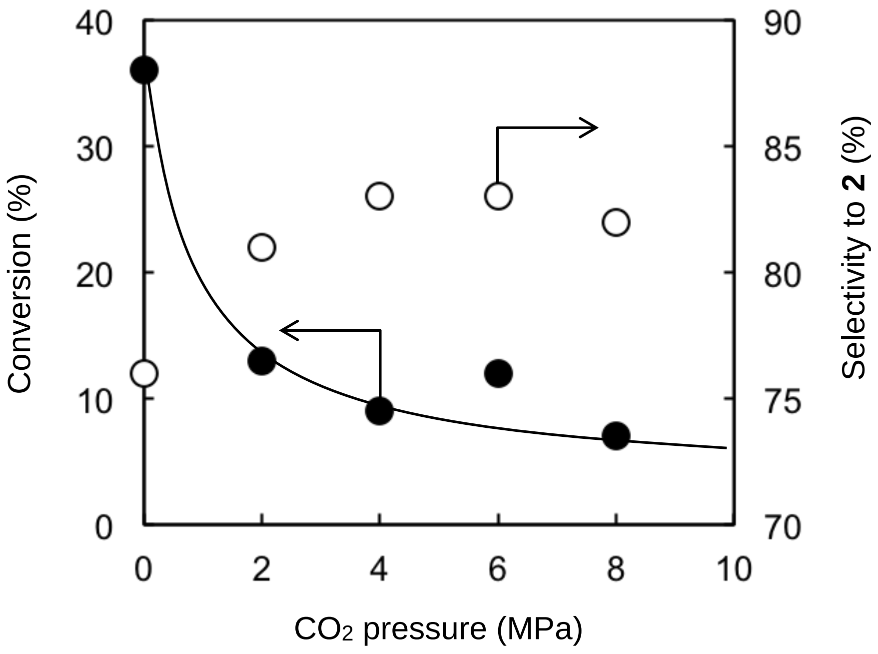

Figure 2. Influence of CO_2 pressure on the overall conversion and the selectivity to **2** in hydrogenation of **1** using 0.5 wt% Pt/TiO_2 for 1 h at 323 K and at a H_2 pressure of 4 MPa.

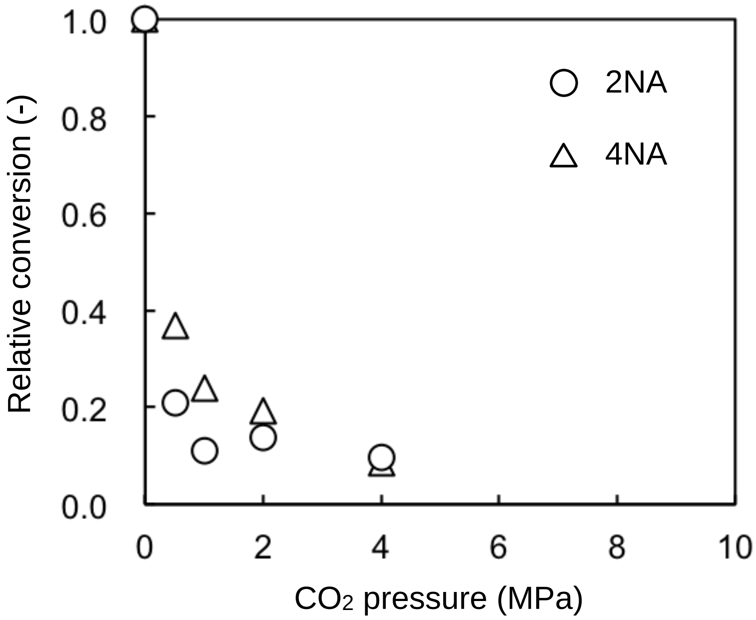

Figure 3. The change of total conversion of 2-nitroaniline (2NA) and 4-nitroaniline (4NA) on CO_2 pressurization at 323 K in the presence of 4 MPa H_2.

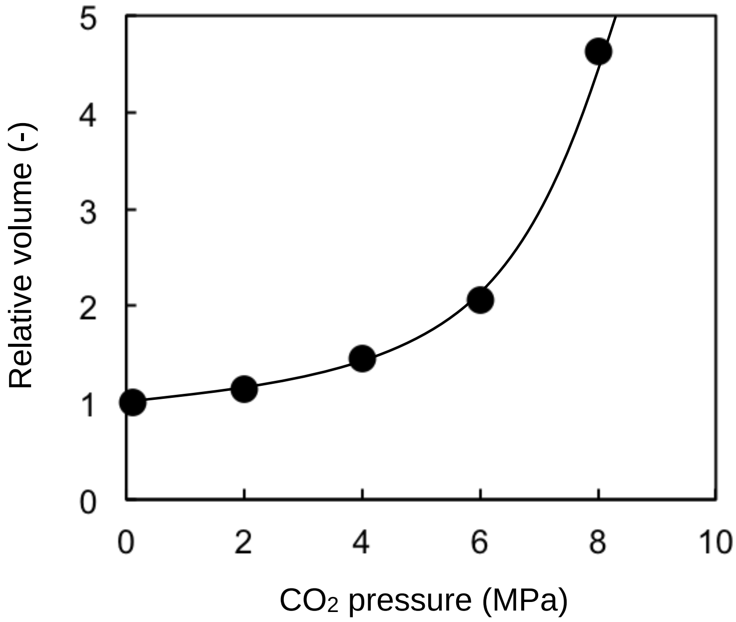

Figure 4. The extent of volume expansion of THF liquid phase on CO_2 pressurization at 323 K in the presence of 4 MPa H_2.

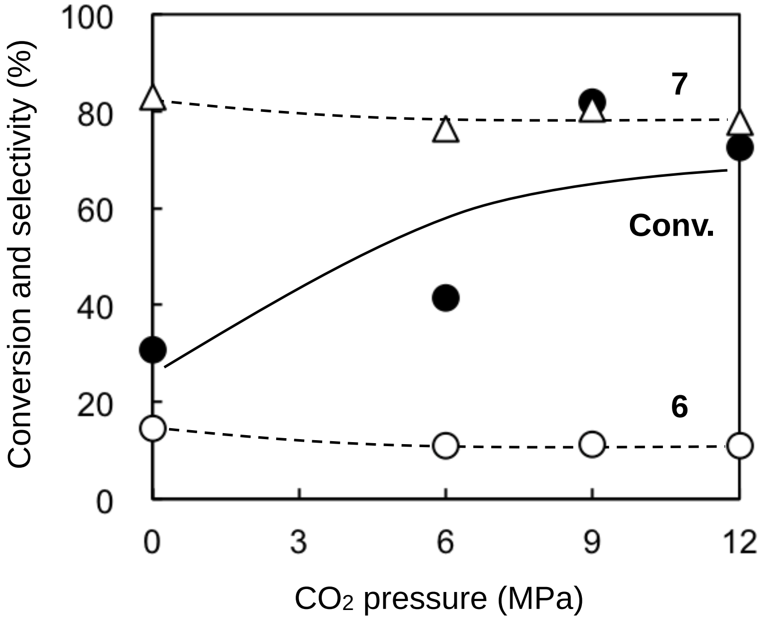

Figure 5. Influence of CO_2 pressure on the overall conversion and selectivity to **6** and **7** in hydrogenation of **5** using 0.5 wt% Pt/TiO_2 for 30 min at 323 K and at a H_2 pressure of 4 MPa.

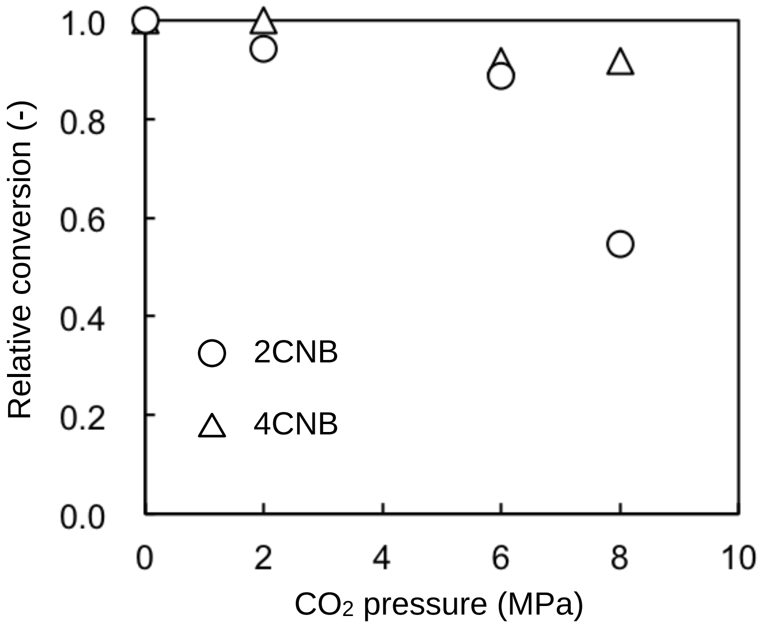

Figure 6. The change of total conversion of 2-chloronitrobenzene (2CNB) and 4-chloronitrobenzene (4CNB) on CO_2 pressurization at 323 K in the presence of 4 MPa H_2.

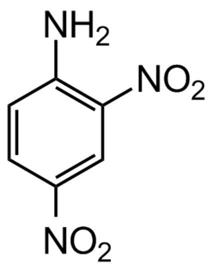

1: 2,4-dinitroaniline

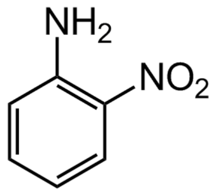

2NA: 2-nitroaniline

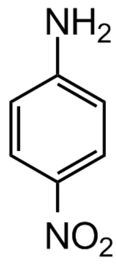

4NA: 4-nitroaniline

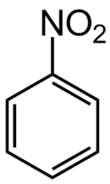

NB: Nitrobenzene

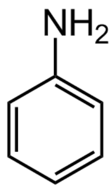

AN: Aniline

Scheme 2. Substrates used for FTIR measurements.

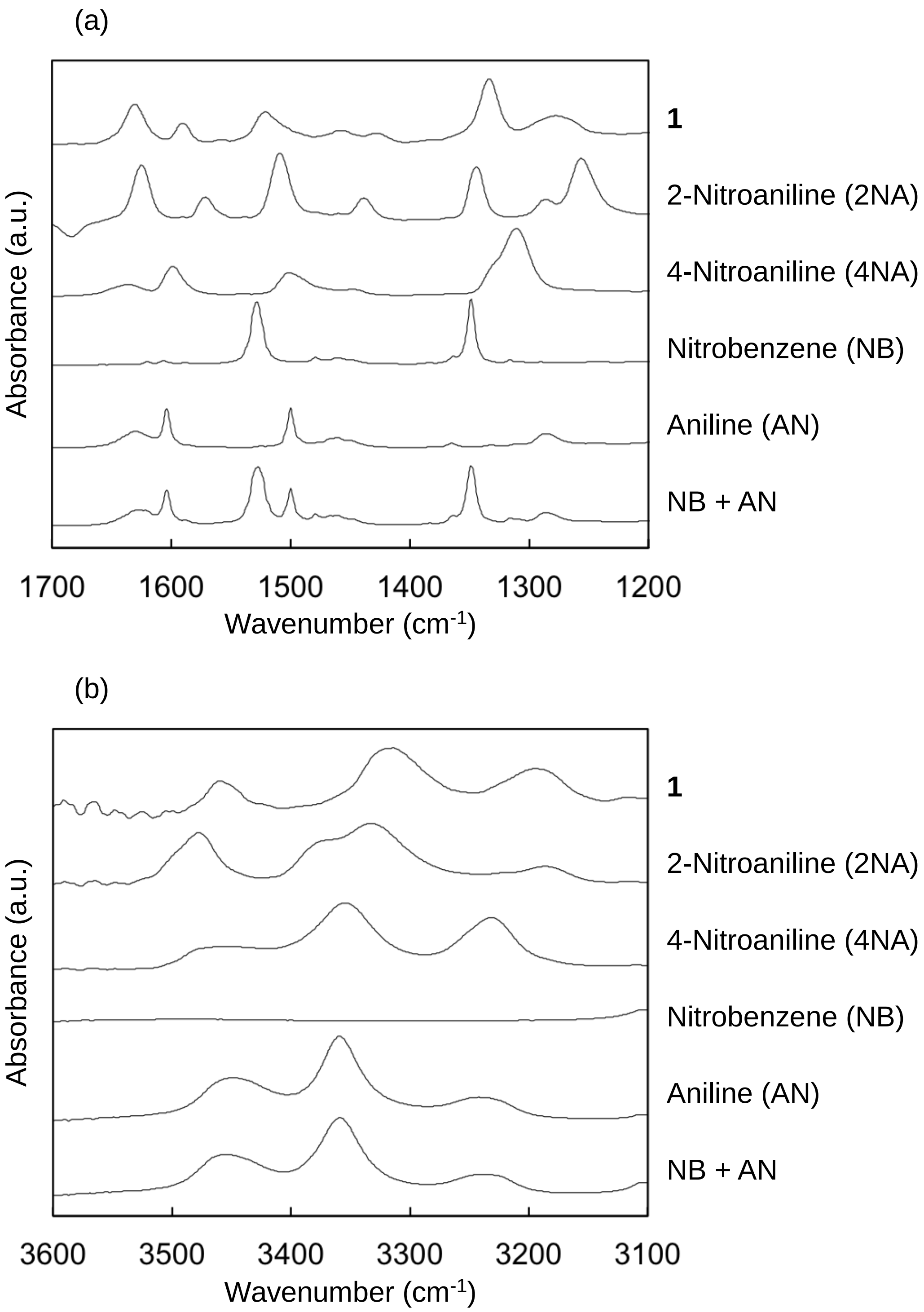

Figure 7. FTIR spectra in the ranges of (a) 1200 – 1700 cm^{-1} (NO_2) and (b) 3100 – 3600 cm^{-1} (NH_2) for 2,4-dinitroaniline **1**, 2-nitroanilline, 4-nitroaniline, nitrobenzene (NB), aniline (AN) and the mixture of NB and AN dissolved in THF measured in transmittance mode under ambient conditions.

Table 1. Assignment of absorption bands observed for **1**, 2NA, 4NA, NB and AN in THF under ambient conditions.

Substrate		$\nu_{as}(NH_2)$	$\nu_s(NH_2)$	$\nu(NH_2)$[a]	$\nu_{as}(NO_2)$	$\nu_s(NO_2)$	$\nu(C\text{-}NH_2)$
1	2-nitro	3453	3312	3185	1513	1329	1272
	4-nitro				1484	1329	
2NA		3471	3326	3177	1505	1340	1251
4NA		3472	3349	3224	1494	1325	1305
NB		-	-	-	1526	1347	-
AN		3444	3353	3232	-	-	1280

[a] Inter-hydrogen bonding

1: 2,4-Dinitroaniline, 2NA: 2-nitroaniline, 4NA: 4-nitroaniline, NB: nitrobenzene, AN: aniline

(a) 2,4-Dinitroaniline **1**

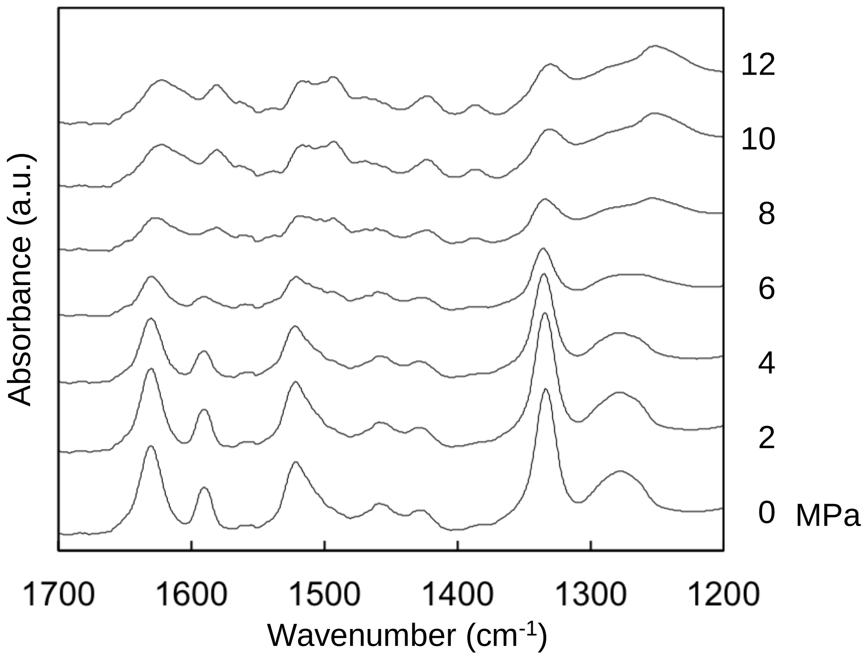

(b) 2-Nitroaniline (2NA)

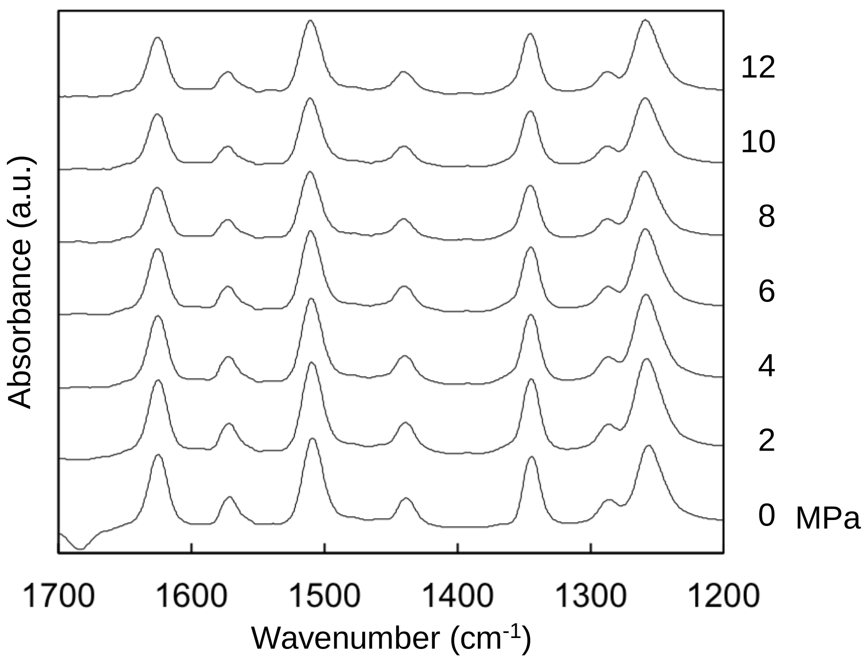

(Figure 8 on pp. 26 & 27)

(c) 4-Nitroaniline (4NA)

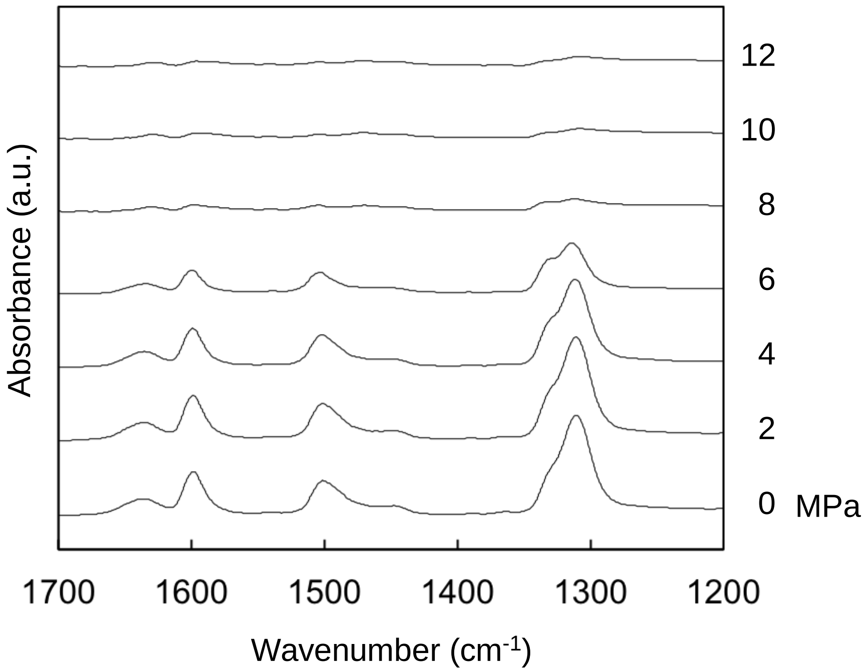

Figure 8. High-pressure FTIR spectra in the range of ν(NO_2) for (a) **1**, (b) 2-nitroaniline and (c) 4-nitroaniline dissolved in THF measured in ATR mode at 323 K at 4 MPa of H_2 and different CO_2 pressures given.

(a) 2,4-Dinitroaniline **1**

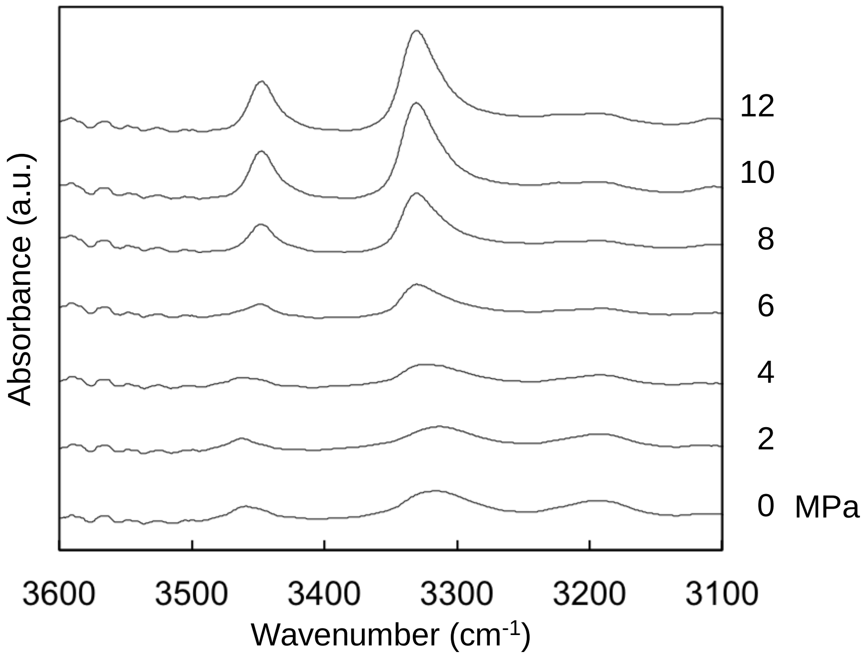

(b) 2-Nitroaniline (2NA)

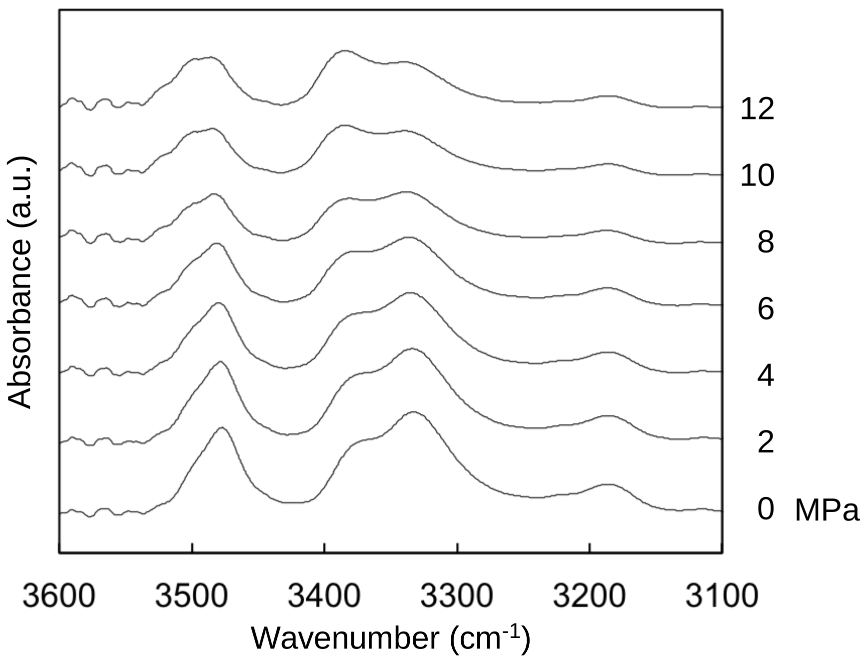

(Figure 9 on pp. 28 & 29)

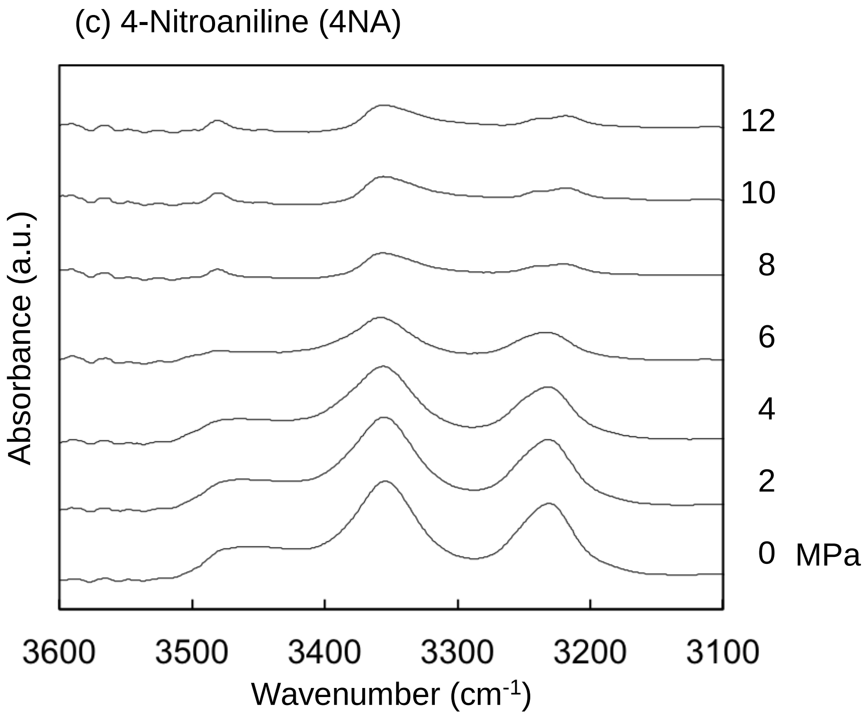

Figure 9. High-pressure FTIR spectra in the range of ν(NH_2) for (a) **1**, (b) 2-nitroaniline and (c) 4-nitroaniline dissolved in THF measured in ATR mode at 323 K at 4 MPa of H_2 and different CO_2 pressures given.

(a) 2,4-Dinitroaniline **1**

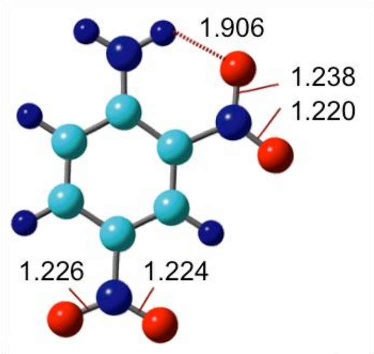

(b) Cluster of **1** with four CO_2 (c) Cluster of **1** with five CO_2

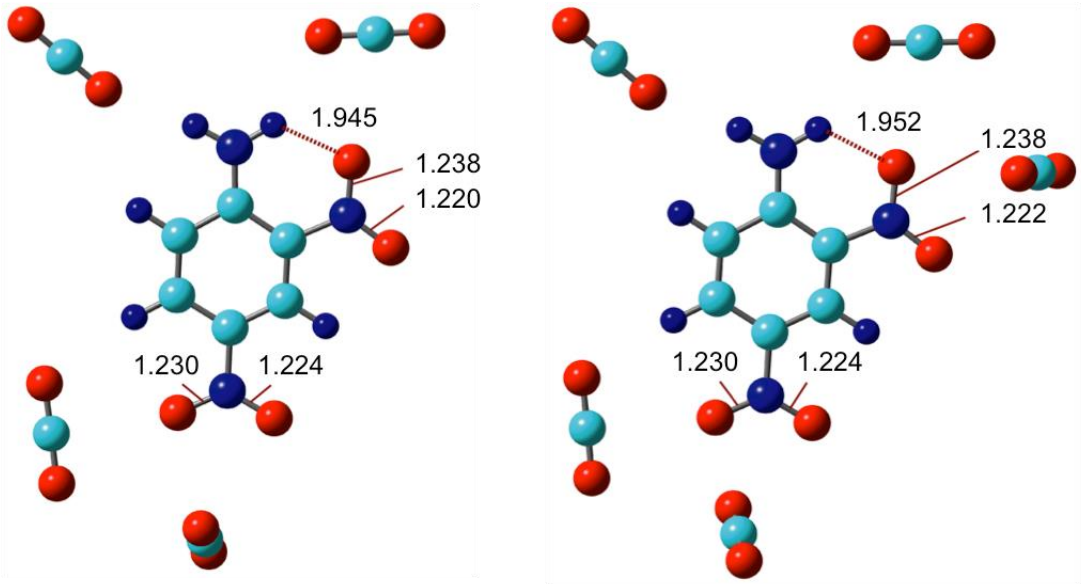

Figure 10. The optimized structures of CO_2-coordinated clusters of **1** with four CO_2 molecules (b) and five CO_2 molecules (c) and the bonding distances of NO of nitro groups and intra-hydrogen bonding between 2-nitro group and amino group in **1**. The values are in Å.

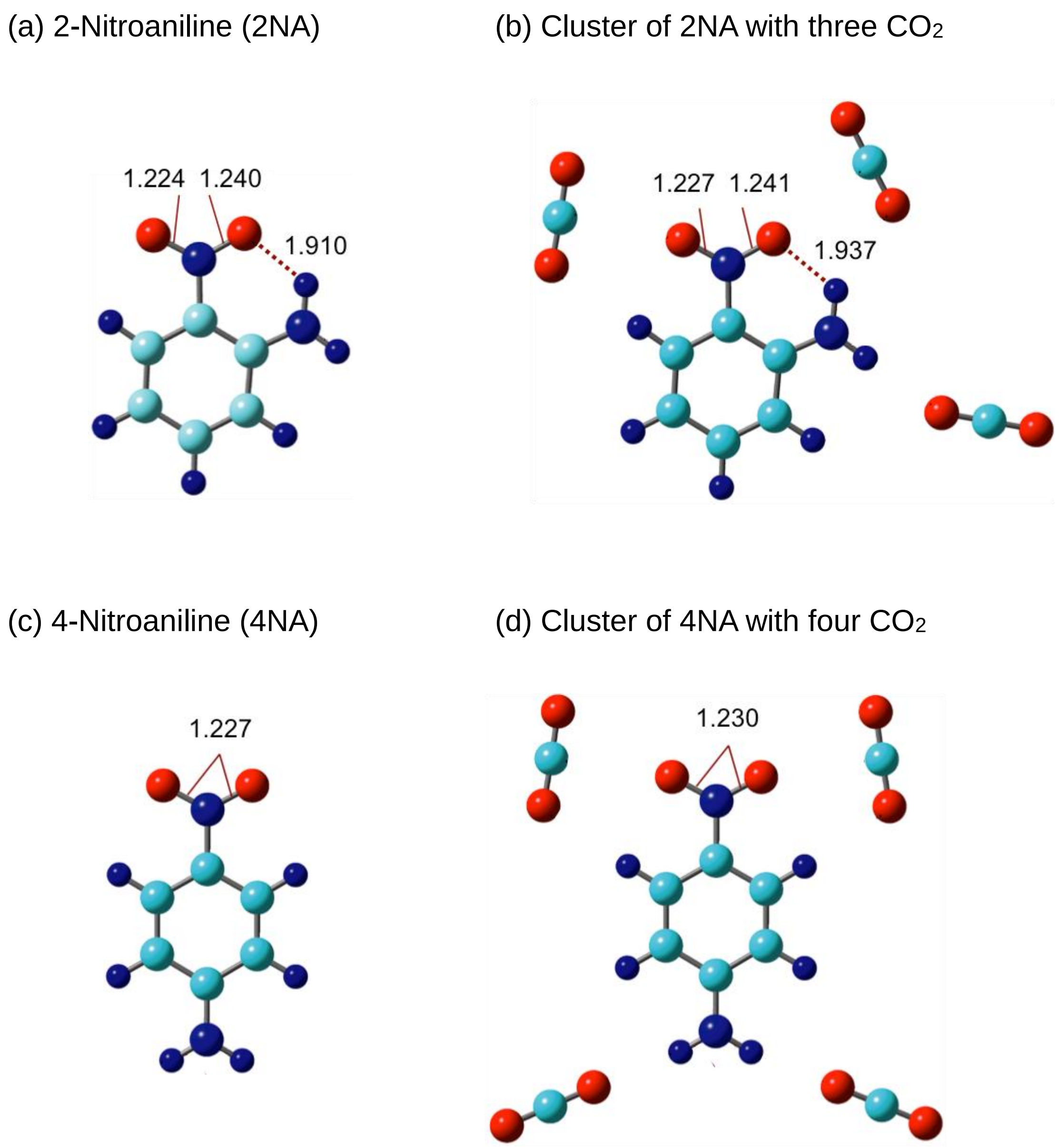

Figure 11. The optimized structures of 2NA (a), CO_2-coordinated clusters of 2NA with three CO_2 molecules (b), 4NA (c), and CO_2-coordinated clusters of 4NA with four CO_2 molecules (d). The bonding distances of NO of nitro groups and intra-hydrogen bonding between 2-nitro group and amino group in 2NA are given in Å.

(a) Dimer of 2NA

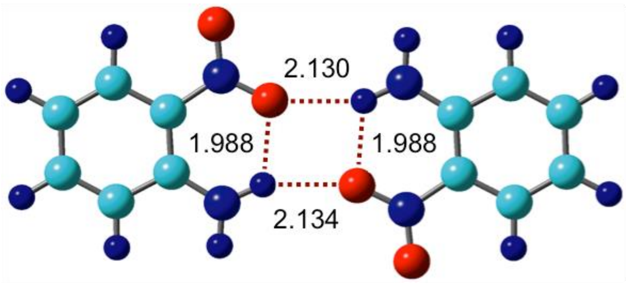

(b) Dimer of 4NA

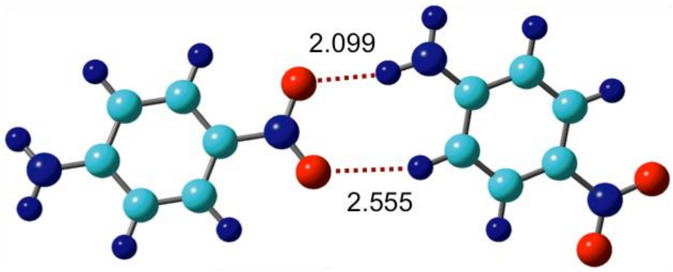

Figure 12. The optimized structures of the dimer of 2NA (a) and 4NA (b). The values of bonding distances are in Å.

(a) Dimer of **1**

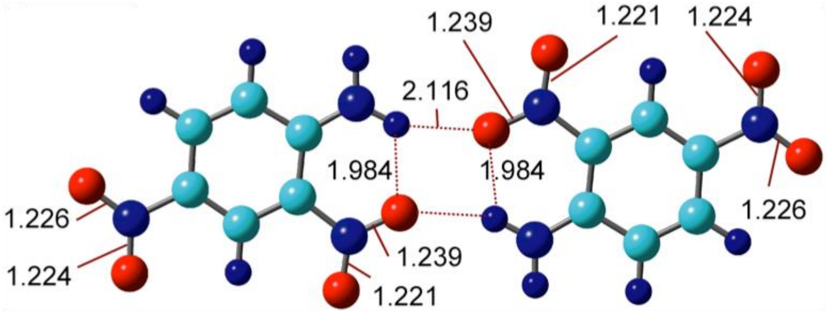

(b) Cluster of Dimer of **1** with eight CO_2

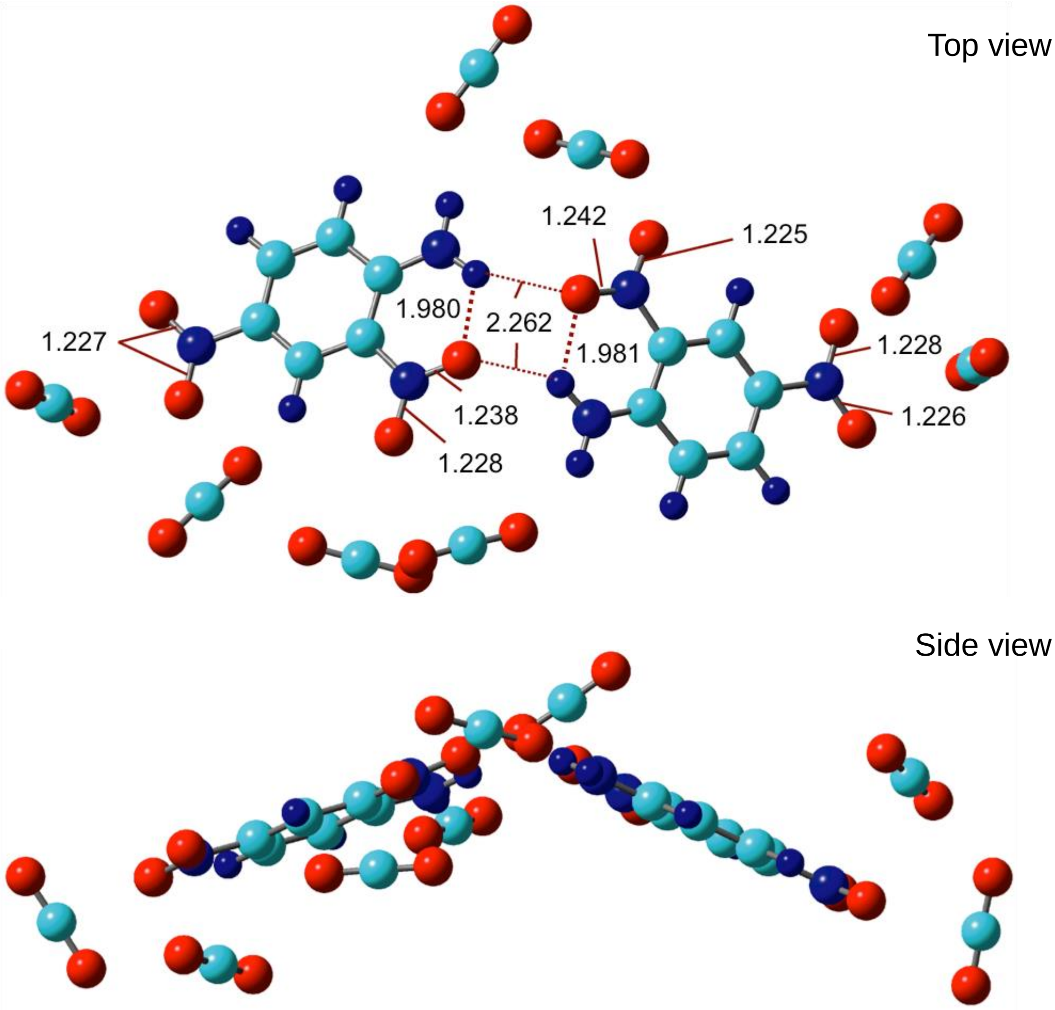

Figure 13. The optimized structures of the dimer of 2,4-dinitroaniline **1** (a) and CO_2-coordinated cluster with eight CO_2 molecules (b). The bonding distances of NO of nitro groups, intra-hydrogen bonding between 2-nitro group and amino group in **1** and inter-hydrogen bonding in the cluster are given in Å.

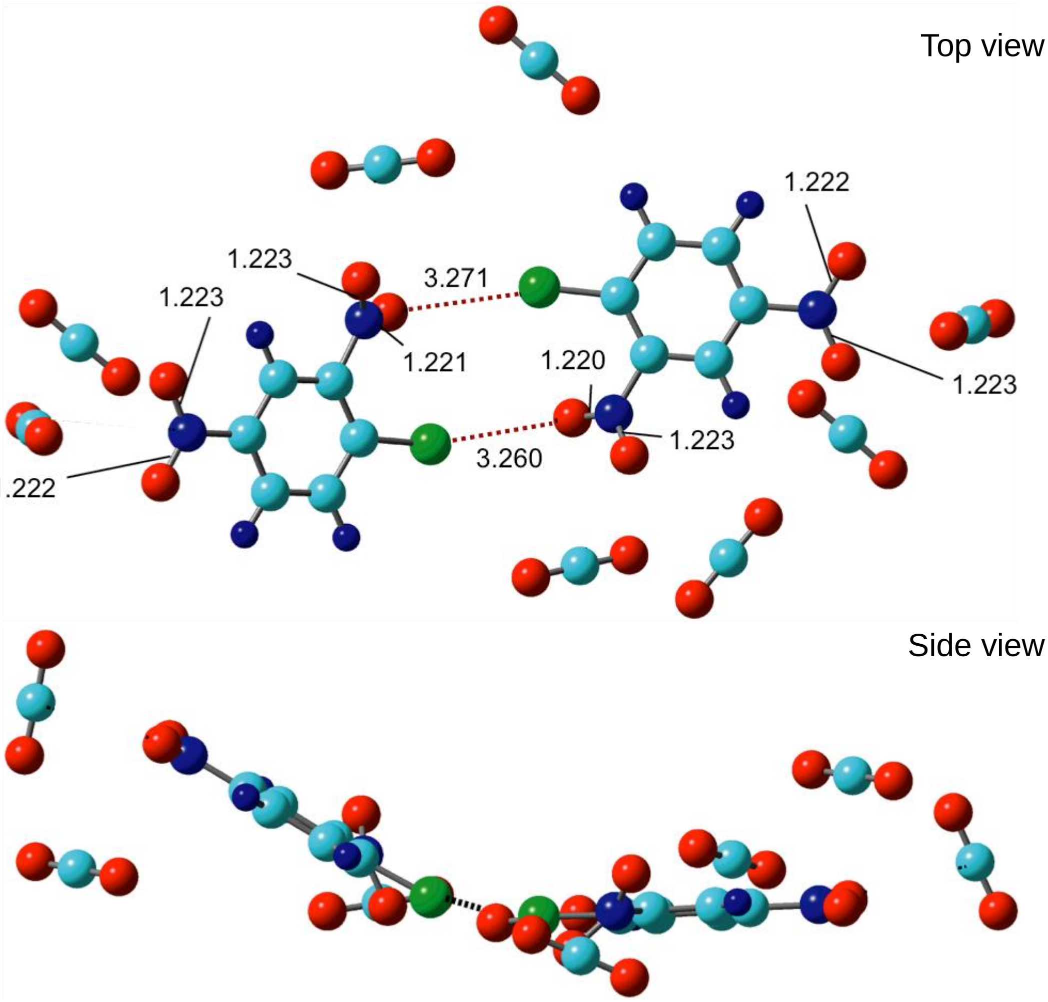

Figure 14. The optimized structures of the dimer of chloro-2,4-dinitrobenzene **5** forming the cluster with eight CO_2 molecules. The bonding distances of NO of nitro groups and the distance between two substrates are given in Å.

.